Surface-enhanced Raman scattering from semi-continuous silver film templates etched by focused ion beams

Bhanu Prakash
Dhamodaran Santhanagopalan

Surface-enhanced Raman scattering from semi-continuous silver film templates etched by focused ion beams

Bhanu Prakash and Dhamodaran Santhanagopalan

Indian Institute of Technology Kanpur, Department of Physics,
Kalyanpur, Kanpur, UP 208016, India
E-mail: dams@iitk.ac.in

Abstract. Semi-continuous silver film templates are fabricated by focused ion beams (FIB), and surface-enhanced Raman scattering spectra from C60-fullerene deposited on these templates are recorded. Films of silver deposited by thermal evaporation are dry-etched by the ion beams with various etching times. The films tend to become semi-continuous as the etch-time increases. The Raman spectra of C60 show an increase in intensity upon correction with a silver coverage area for increasing etch-times. Increase in Raman intensity is due to the sharp edges of the FIB-etched semi-continuous templates, and the moderate enhancements are attributed to dissipation induced by gallium incorporation. A maximum enhancement factor of about 4×10^6 is observed, which is comparable with other experimental values. Controlling gallium incorporation during processing or by post processing treatments is being explored, which can help increase the enhancement factor.

Subject terms: focused ion beams; semi-continuous silver films; C60-fullerene; surface-plasmons, surface-enhanced Raman scattering.

1 INTRODUCTION

The novel plasmonic properties and potential applications of metallic nanostructures have captivated the attention of the scientific community during the past few decades. [1] Nanostructures of metals such as gold and silver that have reasonably low dissipation have been shown to resonantly interact with light over a variety of length-scales, resulting in varied phenomena such as the celebrated extra-ordinary transmission of light, [2] silver super-lenses to focus optical near fields, [3, 4] nano-plasmonic antennas, [5] etc. The two striking features of metallic nanostructures are the extremely large local field enhancements and the drastic modification of the local density of states that becomes possible due to the resonant excitations of the surface plasmons. The large local field enhancements in the nano-structured metal have attracted considerable attention for applications such as templates for surface-enhanced Raman scattering (SERS), [6] and have enabled even Raman sensitivity at the single molecule level. Intensity of the vibrational modes is strongly dependent on wavelengths of lasers used for excitation in Raman spectroscopy. If the wavelength of incident laser is nearly equal to the surface plasmon excitation wavelength, the intensity of the modes is enhanced by a resonant excitation of surface plasmons. Silver and gold are typical metals for SERS experiments, because their plasmon resonance frequencies fall within the visible and near-IR region of electromagnetic spectra with very small dissipation.

Porous and semi-continuous metallic films have been shown to have large amplified local electric fields near the surface through surface plasmon excitation. [7] To generate porous structures, wet chemical etching has been utilized, [8] and it has also been reported that depositing ultrathin metal films can serve as SERS substrates. [9] Although very large local field enhancements of the order of 10^{10} have been theoretically predicted for Raman scattering, [7, 10] measured numbers in terms of enhancement factors tend to be of the order

of 10^4 to 10^7. [9] This raises questions of why large enhancements are not observed in practice. One possibility is that physical vapor deposited and chemically etched porous nanostructures have smoother edges. It is well known that electromagnetically interacting sharp corners with lower symmetries tend to have larger enhancements of local fields compared to interacting smoother metallic surfaces like spherical particles. [11] A highly non-equilibrium dry-etching process, such as with an ion beam, can be used to produce porous and semi-continuous films with sharp features. The focused ion beam (FIB) with its inherent high resolution that results in sharp edges, better processing, and spatial control as well as an isotropic etch, can be utilized for this purpose. But the FIB-based nano-fabrication technique has one notable disadvantage due to the incorporation of gallium (primary beam) into the structures during the fabrication process. [12, 13] Fabrication of semi-continuous metal films by the top down process using FIB for spectroscopic applications is an interesting area to be explored. One possible approach may be Raman spectroscopy, which can be used to acquire information about the vibrational modes of molecules. Hence we were motivated to use dry-etch silver films with FIB to examine their Raman responses. FIB-based dry-etching to fabricate semi-continuous silver films and its SERS response by depositing C60-fullerene on these templates have been investigated. In spite of sharp edges and semi-continuous nature of the templates, the moderate enhancements are attributed to gallium incorporation induced dissipation.

2 EXPERIMENTAL DETAILS

Thin films of silver were deposited on glass substrates using a thermal evaporation system at a pressure of 5×10^{-6} mbar. The thickness of the films was monitored by a quartz crystal thickness monitor, and the thickness of the film was fixed to be approximately 150 nm. FIB-based etching was performed with an FEI (Hillsboro, Oregon) Nova 600 Nanolab dual-beam FIB system, which is comprised of a high-resolution field emission scanning electron microscope (SEM) and a scanning Ga-metal ion beam column. The field emission gallium ion source combined with high resolution (7 nm) ion optics provides high resolution milling. FIB-based dry-etching was carried out for different time intervals by scanning an area of about $140 \times 110 \ \mu m^2$ of the silver films with a 30-keV and 3-nA beam. Pixel by pixel FIB scanning was carried out on a fresh spot for different processing times varying between 1 and 10 min. SEM was used to image the changes in the silver film subsequent to the FIB processing. The fullerene (C60) layer of about 40 nm in thickness was deposited again using a thermal evaporation system before and after generating semi-continuous silver films. Micro-Raman spectra were recorded at room temperature in the back-scattering mode using an Ar-ion laser (514.5 nm) with a spot size of about 12 μm and power of 1 mW. The collection time was 60 sec for all the spectra, and the power density was always less than 1 kW/cm^2 to avoid heating effects.

3 RESULTS AND DISCUSSIONS

Figure 1 shows the SEM images of silver film for FIB-processing times 3, 4, 6, and 10 min, respectively. We could observe from the images that the film tends to become semi-continuous as we increased the processing time. Finally, for longer processing times the film tends to become discontinuous with isolated particles of arbitrary shapes, as shown in Fig. 1(d). It is to be noted that the random semi-continuous films fabricated by FIB appear to have comparatively sharp edges, which could be important for SERS applications where local field enhancements are large. Figure 2 shows the Raman spectra (two different frequency regimes) of C60 deposited on plain-glass, as-deposited silver and semi-continuous silver film templates. The observed Raman modes from C60 deposited on glass show small humps with very low intensity, and on silver, a maximum intensity with distinct modes. All observed

modes are identified (Table 1) and compared with different reports on SERS spectra of C60 deposited on silver. [14 – 16]
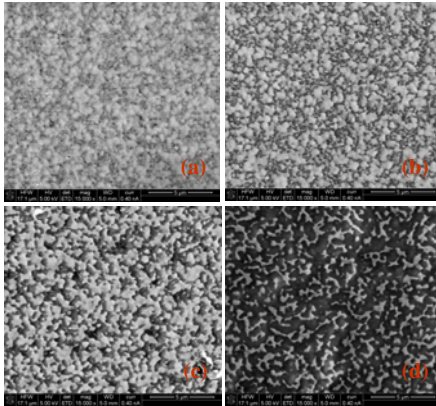

Fig. 1 SEM images of FIB-etched silver films varying etch-time as (a) 3, (b) 4, (c) 6, and (d) 10 min.

Table 1 Observed Raman modes of C60 and their band assignments.

S. No	Raman Shift [14] (cm^{-1})	Raman Shift [15] (cm^{-1})	Raman Shift [16] (cm^{-1})	Present work Raman Shift (cm^{-1})	Assignment (*forbidden modes)
1	268	264	-	263.5	$H_g(1)$
2	430	433	-	427.0	$H_g(2)$
3	492	488	496	487.2	$A_g(1)$
4	530	522	529	519.1	$F_{1u}(1)$*
5	-	-	559	557.7	$H_{1u}(2)$*
6	-	623	-	622.6	$G_g(2)$*
7	708	708	712	705.4	$H_g(3)$
8	772	-	781	771.4	$H_g(4)$
9	-	-	858	857.4	G_g*
10	-	948	-	948.6	A_u*
11	980	971	-	981.8	Higher Order Mode*
12	1424	-	-	1425.6	$H_g(7)$
13	1468	-	1464	1457.2	$A_g(2)$
14	1572	-	1584	1565.0	$H_g(8)$

We observed that predominantly the A_g and H_g modes and the most intense mode was the A_g (2) mode; however, maximum enhancement was observed for H_g (3) mode. Apart from these, F_{1u}, G_g, and A_u modes were also observed in spite of being Raman inactive. It is also important to note that in the present work we have observed greater numbers of such forbidden transitions. The increased number of forbidden modes is attributed to symmetry lowering, molecular distortion, electronic effects, or a combination of all three due to strong C60-silver interfacial interaction. [17] The calculated enhancement factor (the intensity ratio) for A_g (2) and H_g (3) modes for all of the samples is plotted in Fig. 3(a) as a function of FIB-processing time. This plot indicates that maximum enhancement occurs for both H_g (3) and A_g (2) modes for C60 deposited on continuous silver film, and the enhancement factor appears to decrease as a function of FIB-processing time. It is clear from the SEM images (Fig.1) that the grainy structured continuous film transforms into semi-continuous film with nano-particles on a local level with a much lowered coverage of silver. Analysis of the SEM images was performed by converting to binary images, and the coverage area of silver was determined using the ImageJ software. [18] As the FIB-processing time increases, the silver

coverage area decreases, and this would decrease contribution to the Raman scattering. To account for this effect, the enhancement factor was divided by the fraction of the area of silver coverage computed from the SEM images. This is plotted in Fig. 3(b) and shows an increase with FIB-etching time in comparison to Fig. 3(a). The SERS enhancement observed for these modes is due to the surface plasmon resonance of the semi-continuous Ag templates, which couples the incident light into the fullerene molecule very effectively.
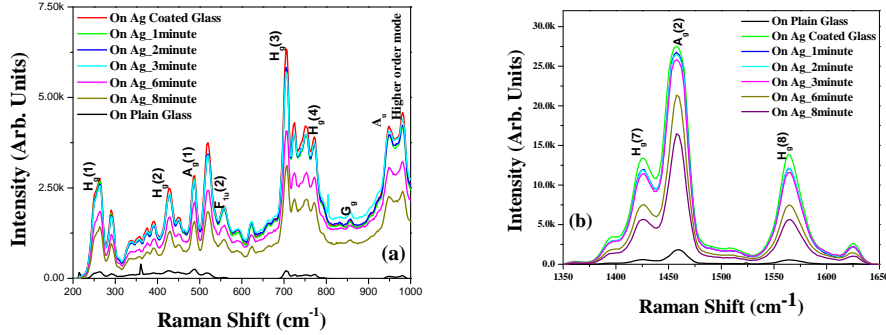

Fig. 2 Raman spectra of fullerene on various templates (a) for the range between 200 cm^{-1} and 1000 cm^{-1}, and (b) for the range between 1350 cm^{-1} and 1650 cm^{-1}. The legends refer to the FIB etching time.
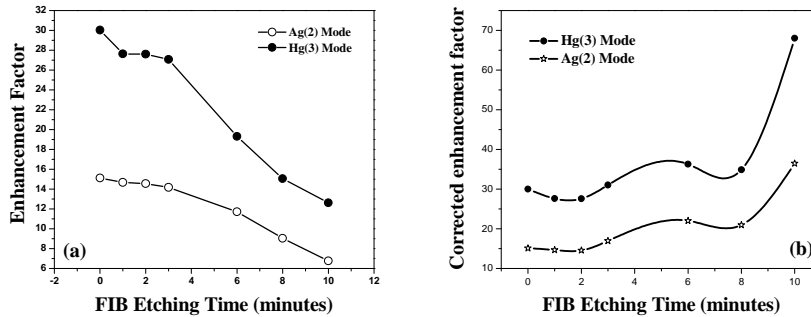

Fig. 3 Raman enhancement factor for the SERS templates (a) for various FIB-etching times and (b) corrected with respect to the coverage area of silver. A_g (2) and H_g (3) refer to the different Raman modes of C60-fullerene.

Figure 3(b) indicates that as a function of FIB-etching time, the enhancement factor is small and moderate for smaller and longer processing times, respectively. The coverage area of silver reduces to less than 1/5 of the initial value, and the corresponding corrected enhancement factor increases only 2.5 times. The possible reasons for the moderate enhancement factors are: 1. for short FIB-processing times, ion beam-induced smoothing of silver film may result in reduced SERS hot-spots, and 2. for long FIB-processing times, the enhancement is not as dramatic as expected due to gallium ion incorporation into the silver films, which is responsible for increased dissipation and the reduced SERS hot-spots. Ion fluence calculated for FIB-processing times range between 6.7×10^{15} ions/cm^2 and 1×10^{17} ions/cm^2 for 1 and 10 min, respectively. Such a high fluence of gallium implantation into the silver films justifies the quenching of surface plasmons due to dissipation. Further studies on the surface plasmon resonance width would be required to quantitatively establish this.

The enhancement factor for silver-based templates prepared by several techniques has been reported to be in the range of 10 to 335, and the maximum effective enhancement factor

in the range of 10^5 to $10^{7.}$ [9, 19 – 24] Only molecules within a very small area around the metallic structures that lie within localized surface plasmon fields contribute to SERS, as pointed out by several groups. With a conservative assumption of an effective volume with a radius of 50 nm (10 nm thickness of C60 film), we have calculated the maximum effective enhancement factor to be 4×10^6 in our case. This value is comparable with other reported values, as shown in Table 2. This factor can be further increased by reducing gallium incorporation-induced dissipation, for example, by further treatments. That will be the focus of future work.

Table 2 Comparison of SERS enhancement factor with several other experiments.

S. No	Template preparation method	Enhancement factor	Max. Effective enhancement factor	Reference
1	Physical vapor deposition	8 – 335	10^7	[9]
2	Physical vapor deposition	150	-	[19]
3	Electro-deposition	33 – 700	-	[20]
4	Electro-deposition	-	$>10^7$	[21]
5	Self-assembly through Langmuir-Blodgett	10 – 100	-	[22]
6	Nano-embossing	-	6.6×10^5	[23]
7	Wet-etching	-	10^7	[24]
8	FIB-etched semi-continuous film	15 – 70	4×10^6	Present work

4 CONCLUSIONS

Fabrication of semi-continuous silver film templates by focused ion beams and control of the film properties by processing time are demonstrated. C60-fullerene deposited on these templates is utilized for investigating the SERS response. The enhancement factor corrected for the coverage area of silver indicates a maximum enhancement for the 10-min FIB-etched template. The moderate enhancement factors are attributed to the smoothing effect at smaller processing times and dissipation induced by gallium incorporation at longer processing times. The enhancement factors reported by several groups are comparable with our experimental value (4×10^6), and this can be further increased by treating the templates. Possibilities of reducing gallium incorporation are being planned, which will be useful for nanophotonic applications.

Acknowledgments

References

[1] S. A. Maier, *Plasmonics: Fundamentals and Applications*, Springer, New York (2007).

[2] W. L. Barnes, A. Dereux, and T. W. Ebbesen, "Surface plasmon subwavelength optics," *Nature* **424**, 824-830 (2003) [doi:10.1038/nature01937].

[3] J. B. Pendry, "Negative refraction makes a perfect lens," *Phys. Rev. Lett.* **85**, 3966-3999 (2000) [doi:10.1103/PhysRevLett.85.3966].

[4] S. A. Ramakrishna, "Physics of negative refractive index materials," *Rep. Prog. Phys.* **68**, 449-521 (2005) [doi:10.1088/0034-4885/68/2/R06].

[5] P. Muhlschlegel, H. -J. Eisler, O. J. F. Martin, B. Hecht, and D. W. Pohl, "Resonant optical antennas," *Science* **308**, 1607-1609 (2005) [doi:10.1126/science.1111886].

[6]   A. Campion, and P. Kambhampati, "Surface-enhanced Raman scattering," *Chem. Soc. Rev.* **27**, 241-250 (1998) [doi:10.1039/a827241z].

[7]   F. Brouers, S. Blacher, A. N. Lagarkov, A. K.Sarychev, P. Gadenne, and V. M. Shalaev, "Theory of giant Raman scattering from semicontinuous films," *Phys. Rev. B* **55**, 13234-13245 (1997) [doi:10.1103/PhysRevB.55.13234].

[8]   S. O. Kucheyev, J. R. Hayes, J. Biener, T. Huser, C. E. Talley, and A. V. Hamza, "Surface-enhanced Raman scattering on nanoporous Au," *Appl. Phys. Lett.* **89**, 53102 (2006) [doi:10.1063/1.2260828].

[9]   R. Kumar, H. Zhou, and S. B. Cronin, "Surface-enhanced Raman spectroscopy and correlated scanning electron microscopy of individual carbon nanotubes," *Appl. Phys. Lett.* **91**, 223105 (2007) [doi:10.1063/1.2816905].

[10]   S. Ducourtieux, V. A. Podolskiy, S. Gre´sillon, S. Buil, B. Berini, P. Gadenne, A. C. Boccara, J. C. Rivoal, W. A. Bragg, K. Banerjee, V. P. Safonov, V. P. Drachev, Z. C. Ying, A. K. Sarychev, and V. M. Shalaev, "Near-field optical studies of semi-continuous metal films," *Phys. Rev. B* **64**, 165403 (2001) [doi:10.1103/PhysRevB.64.165403].

[11]   J. P. Kottmann, O. J. F. Martin, D. R. Smith, and S. Schultz, "Plasmon resonances of silver nanowires with a nonregular cross section," *Phys. Rev. B* **64**, 235402 (2001) [doi:10.1103/PhysRevB.64.235402].

[12]   C. A. Volkert and A.M.Minor, "Focused ion beam microscopy and micromachining," *MRS Bull.* **32**, 389-395 (2007).

[13]   L. Repetto, G. Firpo, and U. Valbusa, "Applications of focused ion beam in materials science," *Mater. Technol.* **42**, 143-149 (2008).

[14]   G. G. Siu, L. Yulong, X. Shishen, X. Jingmei, L. Tiankai, and X. Linge, "Surface-enhanced Raman spectroscopy of monolayer C60 Langmuir-Blodgett films," *Thin Solid Films* **274**, 147-149 (1996) [doi:10.1016/0040-6090(95)07079-6].

[15]   K. L. Akers, L. M. Cousins, and M. Moskovits, "Surface-enhanced vibrational Raman spectroscopy of C60 and C70 on rough silver surfaces," *Chem. Phys. Lett.* **190**, 614-620 (1992) [doi:10.1016/0009-2614(92)85199-K].

[16]   Z. Niu and Y. Fang, "A new surface-enhanced Raman scattering system for C60 fullerene: silver nano-particles/C60/silver film," *Vib. Spectrosc.* **43**, 415-419 (2007) [doi:10.1016/j.vibspec.2006.04.030].

[17]   B. Chase and P. J. Fagan, "Substituted C60 molecules: a study in symmetry reduction," *J. Am. Chem. Soc.* **114**, 2252-2256 (1992) [doi:10.1021/ja00032a048].

[18]   M. D. Abramoff, P. J. Magelhaes, and S. J. Ram, "Image processing with Image J," *Biophoton. Intl.* **11**, 36-42 (2004).

[19]   T. W. H. Oates and S. Noda, "Thickness-gradient dependent Raman enhancement in silver island films," *Appl. Phys. Lett.* **94**, 53106 (2009) [doi:10.1063/1.3078272].

[20]   Y. Yang, A. M. Bittner, and K. Kern, "A new SERS-active sandwich structure," *J. Solid State Electrochem.* **11**, 150 – 154 (2007) [doi:10.1007/s10008-006-0214-z].

[21]   J. Fang, Y. Yi, B. Ding, and X. Song "A route to increase the enhancement factor of surface enhanced Raman scattering (SERS) via a high density Ag flower-like pattern," *Appl. Phys. Lett.* **92**, 131115 (2008) [doi:10.1063/1.2895639].

[22]   Y. Lu, G. L. Liu, and L. P. Lee, "High-density silver nanoparticle film with temperature-controllable interparticle spacing for a tunable surface enhanced Raman scattering substrate," *Nano Lett.* **5**, 5 – 9 (2005) [doi:10.1021/nl048965u].

[23]   D. Jung, Y. M. Lee, Y. Lee, N. H. Kim, K. Kim, and J. K. Lee, "Facile fabrication of large area nanostructures for efficient surface-enhanced Raman scattering," *J. Mater. Chem.* **16**, 3145–3149 (2006) [doi:10.1039/b605480c].

[24]   T. Qiu, Y. Zhou, J. Li, W. Zhang, X. Lang, T. Cui, and P. K. Chu, "Hot spots in highly Raman-enhancing silver nano-dendrites," *J. Phys. D: Appl. Phys.* **42**, 175403 (2009) [doi:10.1088/0022-3727/42/17/175403].